Hindawi
Journal of Sensors
Volume 2023, Article ID 9859804, 1 page
https://doi.org/10.1155/2023/9859804

Retraction

Retracted: Motion Video Image Based on Sensor and Multiprocessing Technology in Track and Field Sports

Journal of Sensors

Received 13 September 2023; Accepted 13 September 2023; Published 14 September 2023

This article has been retracted by Hindawi following an investigation undertaken by the publisher [1]. This investigation has uncovered evidence of one or more of the following indicators of systematic manipulation of the publication process:

(1) Discrepancies in scope
(2) Discrepancies in the description of the research reported
(3) Discrepancies between the availability of data and the research described
(4) Inappropriate citations
(5) Incoherent, meaningless and/or irrelevant content included in the article
(6) Peer-review manipulation

The presence of these indicators undermines our confidence in the integrity of the article's content and we cannot, therefore, vouch for its reliability. Please note that this notice is intended solely to alert readers that the content of this article is unreliable. We have not investigated whether authors were aware of or involved in the systematic manipulation of the publication process.

Wiley and Hindawi regrets that the usual quality checks did not identify these issues before publication and have since put additional measures in place to safeguard research integrity.

We wish to credit our own Research Integrity and Research Publishing teams and anonymous and named external researchers and research integrity experts for contributing to this investigation.

The corresponding author, as the representative of all authors, has been given the opportunity to register their agreement or disagreement to this retraction. We have kept a record of any response received.

References

[1] Z. Tian, "Motion Video Image Based on Sensor and Multiprocessing Technology in Track and Field Sports," *Journal of Sensors*, vol. 2022, Article ID 7651539, 14 pages, 2022.

Hindawi
Journal of Sensors
Volume 2022, Article ID 7651539, 14 pages
https://doi.org/10.1155/2022/7651539

Research Article

Motion Video Image Based on Sensor and Multiprocessing Technology in Track and Field Sports

Zhongxin Tian

College of Physical Education, Taiyuan University of Technology, Taiyuan Shanxi 030024, China

Correspondence should be addressed to Zhongxin Tian; tianzhongxin@tyut.edu.cn

Received 6 July 2022; Revised 6 August 2022; Accepted 9 August 2022; Published 10 September 2022

Academic Editor: Gengxin Sun

In order to use motion video image processing technology to better guide and evaluate athletes' technical and tactical ability, this paper first constructed a motion video image acquisition system. Secondly, a fuzzy kernel estimation method for uniform linear motion based on cepstrum property is proposed. Then, the motion blur areas to be processed are selected, and only these areas are deblurred. Finally, the effective removal of local motion blur is realized, and a clear scene image is obtained. Then, the maximum value of the total entropy of the image is calculated by using the information entropy theory, and the particle swarm optimization algorithm is introduced to find the maximum threshold of image segmentation. Finally, small wave optical flow estimation algorithm and rectangular window scanning algorithm across scales of motion image target detection algorithm are proposed, to not only solve the traditional optical flow estimation for fast moving object detection accuracy but also improve the efficiency of the optical flow computation. Compared to many kinds of algorithms, this paper proposed an algorithm that can improve the accuracy of moving target detection and measurement accuracy. And, the detection accuracy of the proposed algorithm is up to 86.5%. The estimated accuracy was as high as 65%. The segmentation accuracy is up to 95%.

1. Introduction

In order to create ideal competition results, athletes must have good competitive ability and state. Competitive ability is the key factor and fundamental reason for athletes to achieve ideal results [1, 2]. Competitive ability refers to the special ability that athletes must possess in training and competition, which is mainly composed of four basic abilities: physical ability, skill, tactical ability and psychological ability. The application of sports video image multiple processing technology [3, 4] in the field of track and field scientific research is to monitor, analyse, study, and evaluate athletes' physical ability, skill status, and tactical ability, which is an important comprehensive research method and means of physical ability, skill, and combat ability research.

In a broad sense, video image processing technology refers to all kinds of technologies related to video image processing, including physical video image processing technology and related video image processing software and hardware development and application [5, 6]. At present, video image multiple processing technology [7, 8] is used to detect the characters and actions in the movement images collected, which can provide more effective information. Local motion blur in a moving image is caused by the motion of a target objected in the shooting scene. The existing image blur processing technology is devoted to solve the problem of blind and nonblind deblur. Zhu et al. [9] used a statistical distribution model to fit the image blur kernel. Ren et al. [10] pointed out that some strong blurred edges contain rich information, which can be used to assist the estimation of fuzzy kernel and image reconstruction. Feng et al. [11] pointed out that in image reconstruction, normalization constraint on fuzzy kernel can ensure fast convergence of regular optimization model. Gong et al. [12] pointed out that the structural information in the image can be used to estimate the fuzzy kernel. However, these algorithms

can only perform global uniform fuzzy kernel estimation and image deblurring but cannot effectively deblur local motion blurred images. This will cause some difficulties to the subsequent image segmentation. Video image segmentation methods are mainly divided into three categories: video image segmentation methods based on edge [13], region [14], and Canny operator [15]. Moving object detection uses the differences of moving objects in colour, edge, texture, and other aspects in moving image sequence to detect the trajectory of moving objects, extract the contour shape of moving objects, and obtain the position, size, speed, and other moving state information of moving objects. Moving target detection includes identifying whether each moving beacon exists in a specific scene and estimating the motion posture of the moving target. The optical flow method based on differentiation proposed by Tu et al. [16] calculates grayscale differentiation between adjacent image frames, which is relatively simple to achieve and reduce the computational complexity. The disadvantage is that detection errors may occur when the moving target has a large offset. The optical flow method based on matching proposed by Hui et al. [17] can determine the optical flow vector through feature matching of moving targets. This processing method can solve the problem of large difference between adjacent frames, but it cannot solve the problem that the matching algorithm is sensitive to detection noise. The pyramid optical flow method proposed by Zhai et al. [18] can solve the problem that differential optical flow method is only applicable to detection of small moving targets. The main improvement idea of this method is to construct an optical flow pyramid in the existing moving image sequence, and the upper layer is used as the downsampling form of the lower layer after smoothing. However, when the image is decomposed to a certain level, the variation of optical flow of moving objects between adjacent frames becomes very small, which cannot meet the basic requirements of optical flow calculation. A lot of related papers have achieved good results, but detection errors will occur when moving target offset is large. And when the image is decomposed to a certain level, the variation of optical flow of the moving target between adjacent frames will become too small to meet the basic requirements of optical flow calculation.

Based on the above analysis, this paper first constructs a motion video image acquisition system based on sensor technology. Secondly, a detection algorithm for local motion fuzzy region is proposed. The algorithm can detect the fuzzy region and clear region accurately from the local motion blurred image and mark the fuzzy region, so as to deblur the local motion blurred image. Then, in order to meet the needs of computer vision and find the best threshold, a video image segmentation method based on maximum entropy threshold processing algorithm is proposed. The algorithm is based on the image entropy maximization after segmentation to determine the optimal threshold, which meets the requirements of video image segmentation and can improve the accuracy of image segmentation. Finally, the wavelet optical flow estimation algorithm is proposed, and the cross-scale analysis method is applied to the moving target estimation. This algorithm can accurately estimate the moving targets with different rates in the same moving scene and solves the problem that the detection accuracy of the fast moving targets is reduced by the traditional optical flow estimation.

2. Motion Video Image Acquisition System

Figure 1 shows the overall architecture of the motion video image acquisition system designed in this paper. Through video acquisition and storage technology, the most basic video image information source is processed without disturbing the sports scene, and then, different technical methods are adopted to analyze and evaluate the technical and tactical abilities of athletes in different events. The principle and process of video image processing technology are complex and diverse. In the field of track and field scientific research, we only need to understand and master its functions and application methods. Video image processing system consists of video image acquisition equipment, video image transmission equipment, video image storage equipment, video image processing equipment, video image demonstration equipment, and a series of software and hardware. Only when the basic configuration of video image processing technology is satisfied, the corresponding video image processing and analysis can be carried out.

The system is mainly composed of ARM core processor, video acquisition equipment, PC, and other parts. ARM microprocessor controls the collection and transmission of video data, and the PC displays the collected data as the client and builds the human-computer interaction interface. Meanwhile, the image processing module is developed on the computer platform.

According to the software and hardware configuration requirements of the video image, the Linux operating platform is adopted, and the random RAM is 1 GB with CPU frequency PIII of 8500 MHz or more. The resolution is set to 1024×768 and is 24-bit (or 32-bit) true colour. High-speed video image acquisition with built-in IEEE1394 interface.

Video capture device uses USB camera, and ARM processor directly uses USB bus communication for plug and play, which simple and convenient. ARM processor is the data acquisition server and the core module of the whole embedded system. It completes the configuration of server hardware with power management module, memory module, SDRAM, and network interface. The video server collects data and transmits it to the PC client browser through twisted-pair cable. The client develops on the PC and connects the system to the network on Linux. This allows each node in the network to access the server. At the same time, a processing application based on VC++ was developed, and the image processing interface of the system was designed, including opening the image, image deblurring, and target detection.

System hardware includes embedded processor and peripheral devices. Embedded microcontroller processor is the core component of embedded system; it has the biggest difference between embedded processor in the field specially designed for specific occasions and special system. The most in common processor by the board to complete

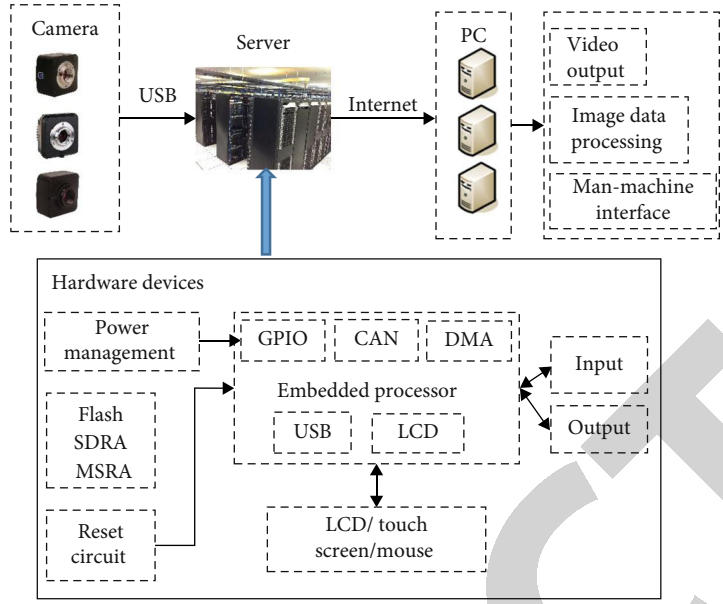

Figure 1: This paper designs the overall architecture of the motion video image acquisition system.

the task of integration to the interior of the processor chip; it can meet the requirements of miniaturization, high efficiency, reliability, and real time of embedded system. In different application fields and different development stages of embedded system, the embedded system software is not completely the same. In many fields, the embedded system software does not use the same structure as the general computer.

The running flow chart of the data acquisition process is shown in Figure 2.

3. Multiprocessing Algorithm for Moving Video Images

3.1. Motion Image Deblurring Algorithm (DA). Generally, image processing methods are divided into spatial domain method and frequency domain method. The spatial domain method has a large amount of data in image processing, which is difficult to achieve, especially for fuzzy image deblurring. Frequency domain method uses positive and negative Fourier transform for image processing, which reduces the amount of data and improves the processing accuracy.

Spatial domain method processing fuzzy image has a large amount of data and is difficult to meet the basic requirements of edge feature extraction. However, in the frequency domain, there are significant differences between the clear image and the moving image. For example, the texture features of the clear image are clear and relatively smooth, and some special zeros appear in the moving blurred image in the frequency domain, which are associated with the features of the moving blurred image.

This section makes use of the spectrum feature to analyse the frequency domain feature of motion blur image. In a linear time-invariant system, the time-domain expression of point diffusion function of uniformly linear moving images is

$$\lim(a,b) = \frac{1}{L}, \quad \text{if } \left(a^2 + b^2 < \frac{L}{2}, \frac{a}{b} = -\tan\theta\right). \tag{1}$$

Assuming that the fuzzy image moves horizontally and the size is $M * N$, according to the expression $g(x,y) = f(x,y) * h(x,y) + n(x,y)$, it can be known that the point diffusion function $M * N$ is also $M *$ matrix, and the zero-filling expansion is carried out. The c matrix expression is

$$\lim(a,b) = \begin{pmatrix} 1/L & 1/L & \cdots & 0 \\ \cdots & \cdots & \cdots & \cdots \\ 0 & 0 & 0 & 0 \end{pmatrix}. \tag{2}$$

Two-dimensional Fourier transform is applied to it, and the expression of point diffusion function in frequency domain of uniformly linear motion image can be obtained:

$$\lim\left(a', b'\right) = \sum \lim(a,b) e^{-2*\left(\left(a*a'/N\right)+\left(b*b'/M\right)\right)}. \tag{3}$$

By quantitative analysis of a' and b', respectively, it can be seen that the two-dimensional Fourier transform spectrum of motion fuzzy image contains the direction and length characteristics of fuzzy kernel. Therefore, spectrum characteristics can be extracted and analysed, and the fuzzy angle and fuzzy scale can be estimated by mathematical method.

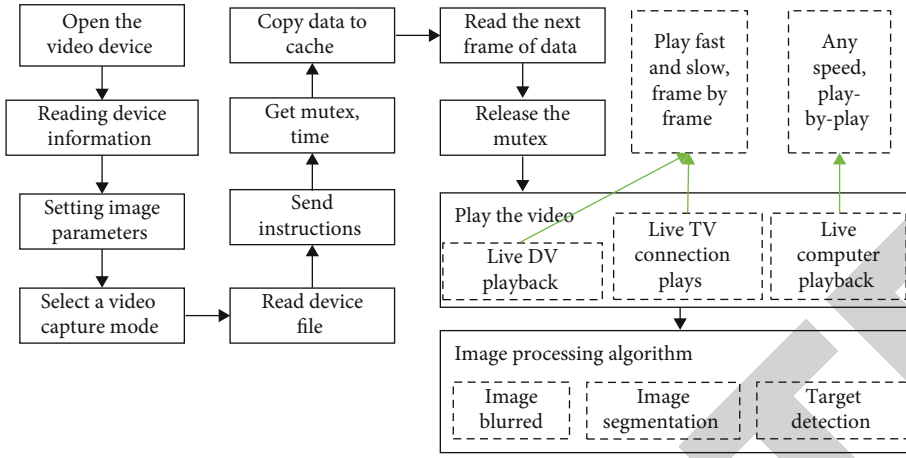

Figure 2: The process of collecting motion video images.

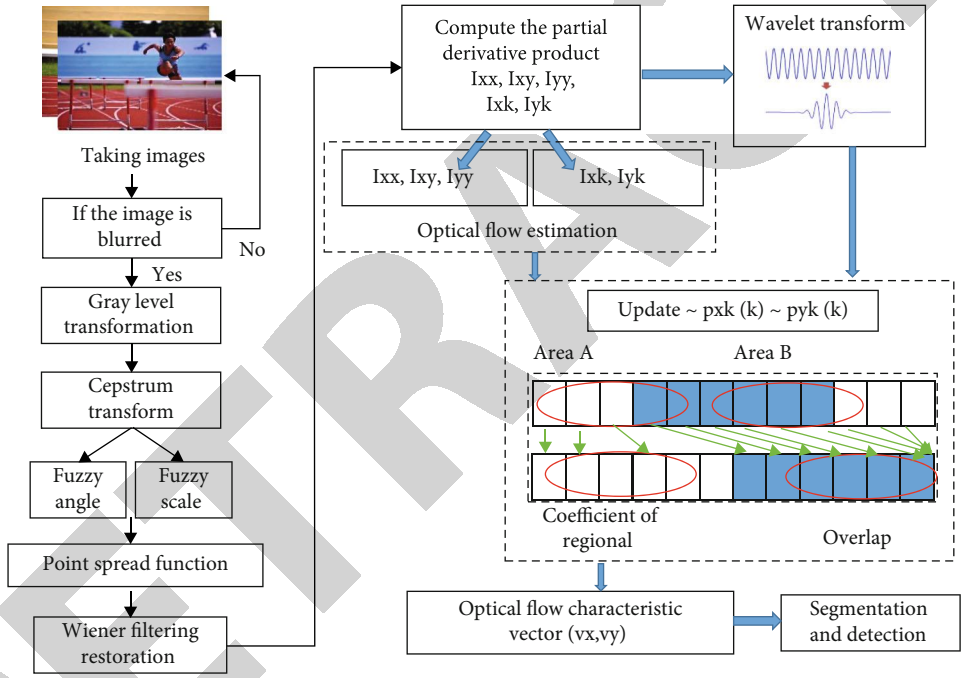

Figure 3: Target detection algorithm for cross-scale moving images.

The cepstrum definition of motion blur image $\mathrm{blu}(x, y)$ is described mathematically as follows:

$$\mathrm{blu}(u, v) = F^{-1} * (\log |\mathrm{blu}(x, y)|), \tag{4}$$

where F^{-1} is the two-dimensional inverse Fourier transform.

In order to extract fuzzy information and estimate fuzzy kernel more accurately based on cepstrum characteristics, Canny operator is used to detect the precise edge of cepstrum. Canny operator uses the derivative characteristics of Gaussian function to detect the optimal edge. It has the characteristics of antinoise, fast operation, and high-precision edge detection.

Canny believes that Gaussian filtering is optimal for edge detection. The mathematical expression of Gaussian operator is

$$G(a, b, \sigma) = e^{-\left(x^2+y^2\right)/2\sigma^2}. \tag{5}$$

After differential treatment, it can be expressed as

$$dG(a, b, \sigma) = \frac{dG(a, b, \sigma)}{da} U_a + \frac{dG(a, b, \sigma)}{db} U_b, \tag{6}$$

where U_a and U_b are unit vectors.

The specific steps of the fuzzy kernel estimation algorithm based on cepstrum characteristics are as follows:

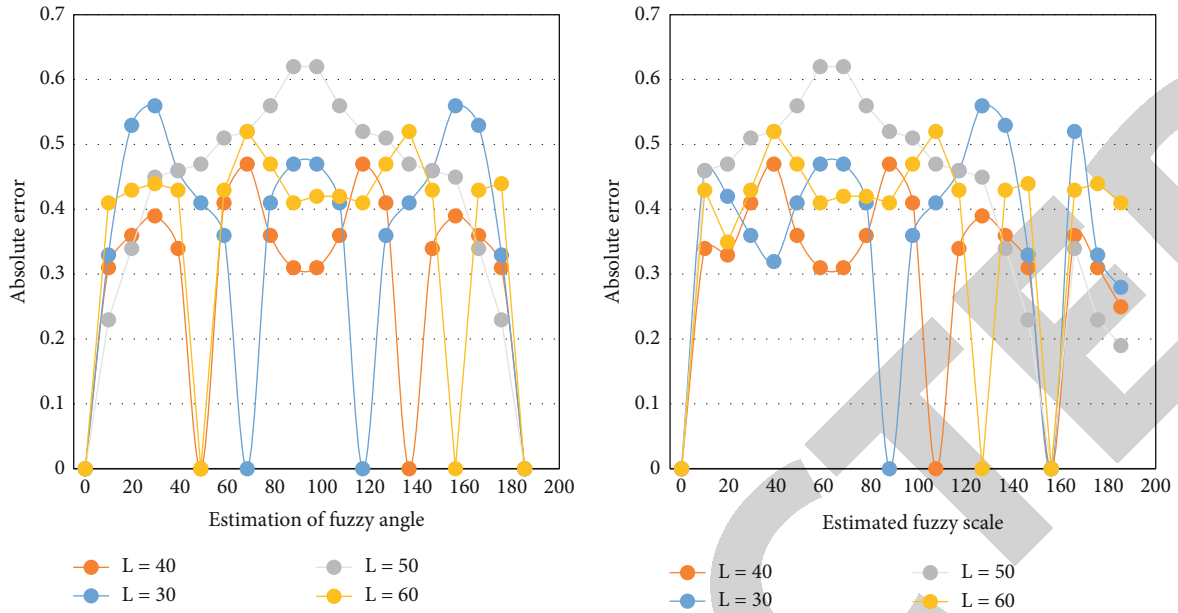

(a) Absolute error of fuzzy angle

(b) Fuzzy scale absolute error

Figure 4: Error comparison.

Table 1: Experimental results of motion blur images without noise.

Data (L/θ)	Estimated fuzzy kernel (L/θ)			Absolute error (L/θ)		
	1st image	2nd image	3rd image	1st image	2nd image	3rd image
5/10	5/0	5/0	5/0	0/0	0/0	0/0
5/30	5.6/31.1	5.6/31.1	5.6/31.1	0.8/1.1	0.8/1.1	0.8/1.1
10/10	10.2/11.3	10.2/11.3	10.2/11.3	0.2/1.3	0.2/1.3	0.2/1.3
10/30	10.3/29.1	10.3/29.1	10.3/29.1	0.3/0.9	0.3/0.9	0.3/0.9
30/10	10.1/11.1	10.1/11.1	10.1/11.1	0.6/1.2	0.6/1.2	0.6/1.2
30/30	30/30	30/30	30/30	0/0	0/0	0/0

(1) Two-dimensional Fourier transform is performed on the motion blurred image $\mathrm{blu}(x, y)$ to obtain the spectrum $\mathrm{blu}(u, v)$

(2) The spectral graph $\mathrm{blu}(u, v)$ is logarithmically processed, and then, the two-dimensional inverse Fourier transform is performed to obtain $\mathrm{blu}(u', v')$, which migrates $u = 0$ and $v = 0$ to the centre to obtain blu $(u', v')'$

(3) For cepstrum $\mathrm{blu}(u', v')'$, Canny edge detection was carried out by using the above method, and the cepstrum edge detection graph was obtained

(4) Using cepstrum symmetry, set the grey value of the left half plane of the cepstrum graph to 0 to obtain a maximum negative peak p

(5) Set the grey value of the right half plane of the cepstrum graph to 0 to obtain another maximum negative peak q

(6) Using the distance between the maximum negative peak points to be two times of the fuzzy scale,

$$L = \frac{1}{2} * \left((p_1 - p_2)^2 + (q_1 - q_2)^2\right)^{1/2} \quad (7)$$

(7) Using the angle between the maximum negative peak points to find the fuzzy angle,

$$\theta = 180/\pi * ac\tan\left((p_1 - p_2)/(q_1 - q_2)\right) \quad (8)$$

3.2. Maximum Entropy Processing Segmentation Algorithm for Video Images (MEPSA). Based on the above deblurred video image, the unknown threshold is set as k, and the total entropy of the image s is calculated. Assume that there are M pixel values in the video image. According to the concept of information entropy, the information entropy corresponding to each pixel is expressed as

$$H = -\sum p_x \log p_x, \qquad p_x = \frac{q_x}{M}. \quad (9)$$

In the above formula, H represents the information entropy corresponding to pixel point; p_x represents the probability of each grey level x appearing in the video image. q_x represents the number of pixels with a grey value of x. Probability distribution of each pixel in each region is shown

Table 2: Experimental results of motion blur images with Gaussian noise with mean value of 0 and mean square error of 0.001.

Data (L/θ)	Estimated fuzzy kernel (L/θ)			Absolute error (L/θ)		
	1st image	2nd image	3rd image	1st image	2nd image	3rd image
5/10	6.1/9.5	6.1/9.5	6.1/9.5	6.1/9.5	6.1/9.5	6.1/9.5
5/30	5.4/21.8	5.4/21.8	5.4/21.8	0.4/8.2	0.4/8.2	0.4/8.2
10/10	10.2/11.3	10.2/11.3	10.2/11.3	0.2/1.3	0.2/1.3	0.2/1.3
10/30	10.3/29.1	10.3/29.1	10.3/29.1	0.3/0.9	0.3/0.9	0.3/0.9
30/10	30.9/11.1	30.9/11.1	30.9/11.1	0.9/0.9	0.9/0.9	0.9/0.9
30/30	30.9/29.1	30.9/29.1	30.9/29.1	0.2/0.4	0.2/0.4	0.2/0.4

Table 3: Experimental results of motion blur images with Gaussian noise with mean value of 0 and mean square error of 0.00001.

Data (L/θ)	Estimated fuzzy kernel (L/θ)			Absolute error (L/θ)		
	1st image	2nd image	3rd image	1st image	2nd image	3rd image
5/10	5/0	5/0	5/0	0/0	0/0	0/0
5/30	5.1/29.8	5.1/29.8	5.1/29.8	0.1/1.3	0.1/1.3	0.1/1.3
10/10	10.2/11.3	10.2/11.3	10.2/11.3	0.2/1.3	0.2/1.3	0.2/1.3
10/30	10.3/29.1	10.3/29.1	10.3/29.1	0.3/0.9	0.3/0.9	0.3/0.9
30/10	30.1/9.8	30.1/9.8	30.1/9.8	0.6/1.2	0.6/1.2	0.6/1.2
30/30	30/30	30/30	30/30	0/0	0/0	0/0

in the formula below:

$$A : \frac{p_0}{p_1}, \frac{p_1}{p_2}, \cdots, \frac{p_k}{p_k},$$
$$B : \frac{p_{k+1}}{1-p_1}, \frac{p_{k+2}}{1-p_2}, \cdots, \frac{p_{k+M}}{1-p_k}. \tag{10}$$

Then, the sum of information entropy of region A and region B can be calculated by

$$H_A(k) = \sum \frac{p_x}{p_k} \log \frac{p_x}{p_k}, \tag{11}$$

$$H_B(k) = \sum \frac{p_x}{1-p_k} \log \frac{p_x}{1-p_k}. \tag{12}$$

In Equations (11) and (12), $H_A(k)$ and $H_B(k)$ represent the sum of information entropy of region A and region B, respectively. By adding the results in formula (11) and formula (12), the total entropy of characters in the video image can be obtained, which is expressed as

$$H_A(k) = \log p_k(1-p_k) + \frac{H(k)}{p_k} + \frac{H - H(k)}{1-p_k}. \tag{13}$$

Through the above process, the total entropy of the video image is calculated.

Taking the maximum value of the total entropy $H(k)$ of the image as the target, the threshold k solved is the optimal threshold of video image character segmentation. It can be seen that the solution process of the optimal threshold is equivalent to the function optimization problem, and the calculation process is complicated. In order to simplify the solution process of the optimal threshold, particle swarm optimization algorithm is introduced to solve the optimal threshold of video image segmentation. It is found that particle swarm optimization algorithm can solve the continuous optimization problem which has high accuracy and efficiency, which can greatly reduce the time consumed in calculating the optimal threshold value and improve the performance of video image segmentation method.

3.3. Target Detection of Cross-Scale Moving Images. In this section, the target detection algorithm of cross-scale moving image is integrated with wavelet optical flow estimation algorithm and linear and rectangular window scanning algorithm. The wavelet optical flow estimation algorithm can accurately estimate the moving targets with different moving rates in the same moving scene, which solves the problem that the traditional optical flow estimation has low detection accuracy for fast moving targets, reduces the complexity of optical flow calculation, and improves the efficiency of optical flow estimation. The rectangular window scanning algorithm realizes the adaptive adjustment of target detection and can realize continuous cross-scale moving image target detection between moving image interval frames. The framework structure of the algorithm is shown in Figure 3.

$I(x, y, k)$ represents the brightness value of pixel point (x, y) at time point k. Brightness constancy assumes that image sequence $I(x, y, k)$ will not change significantly in a short period of time. I_x, I_y, and I_k are partial derivatives of $I(x, y, k)$ with respect to x, y, k, and (vx, vy) are velocity vectors of optical flow term $I(x, y, k)$. According to the brightness constancy hypothesis, $(v \text{ such as } y)$ is set to be constant in a small range, so the optical flow equation can be defined as

$$I(x, y, k) = \Delta I(x + u, y + v, k). \tag{14}$$

Wavelet optical flow estimation algorithm (WOF) adaptively determines the parameter r by the optical flow amplitude. By applying wavelet transform to the optical flow estimation algorithm, the optical flow equation can be rewritten as

$$\text{WOF} = \iint \left\{ {I_x}^2 a^2 + {I_y}^2 b^2 + {I_k}^2 + 2I_x I_x ab + 2I_x I_x \text{a} + 2I_x I_x b \right\} dxdy. \tag{15}$$

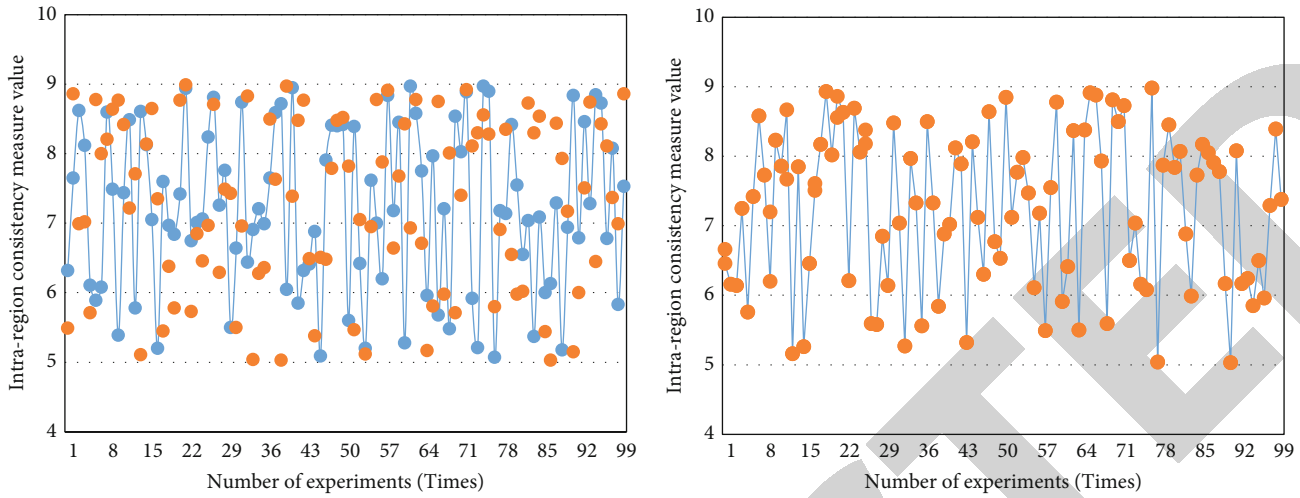

(a) Consistency measurement results in noisy environment

(b) Consistency measurement results in non-noisy environment

Figure 5: Results of intraregion consistency measure under different conditions.

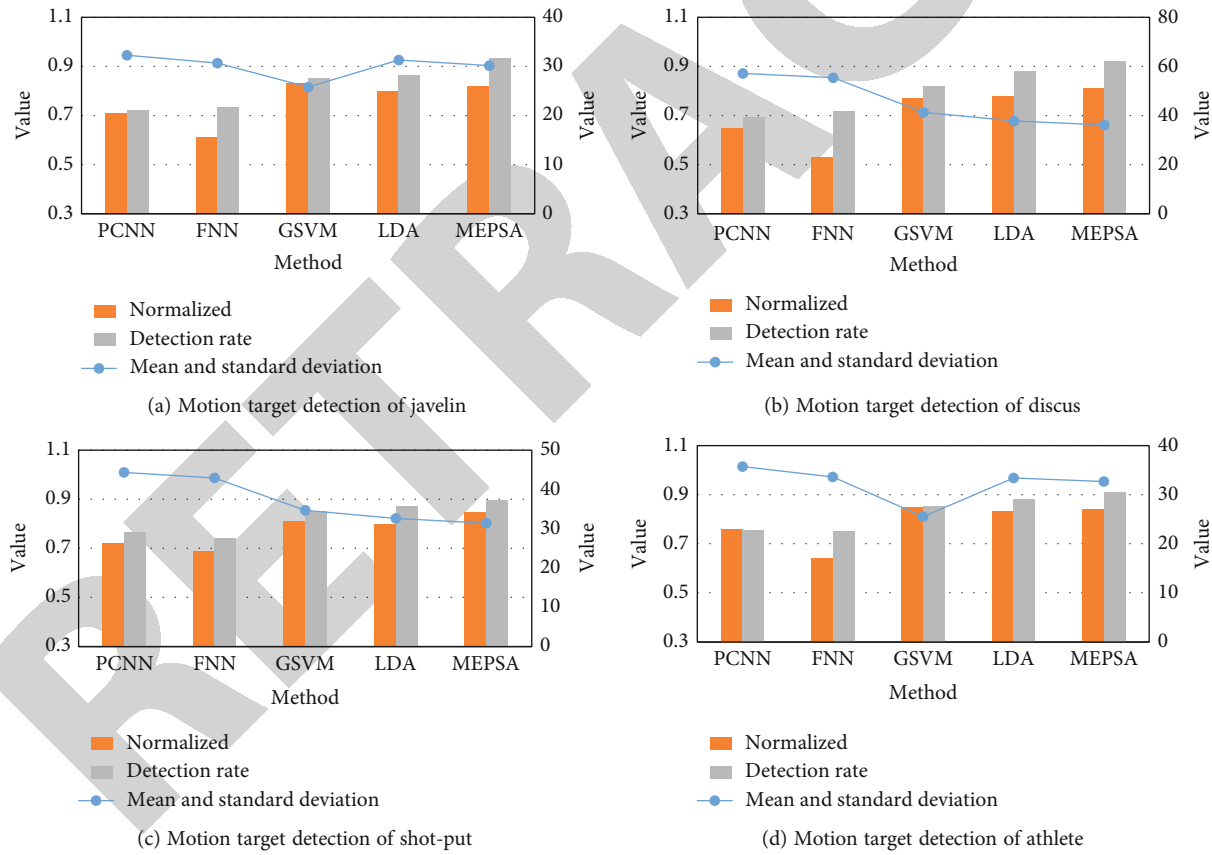

(a) Motion target detection of javelin

(b) Motion target detection of discus

(c) Motion target detection of shot-put

(d) Motion target detection of athlete

Figure 6: Experimental results of different segmentation algorithms.

In order to accurately detect the moving target from the image, the moving target detection algorithm needs to determine the rectangular window with the scale of $M \times N$. Existing moving target detection algorithm according to the characteristics of the moving targets using sequential scan mode. But in the process of sequential scan, moving target area detection cannot adaptive adjustment. In addition, between different frames, moving object detection will appear. The same moving target may be detected as different moving target regions, and these defects will affect the final moving target detection results.

In this section, a rectangle window scan (RWS) algorithm is proposed. RWS algorithm can realize adaptive adjustment of moving object detection and can realize

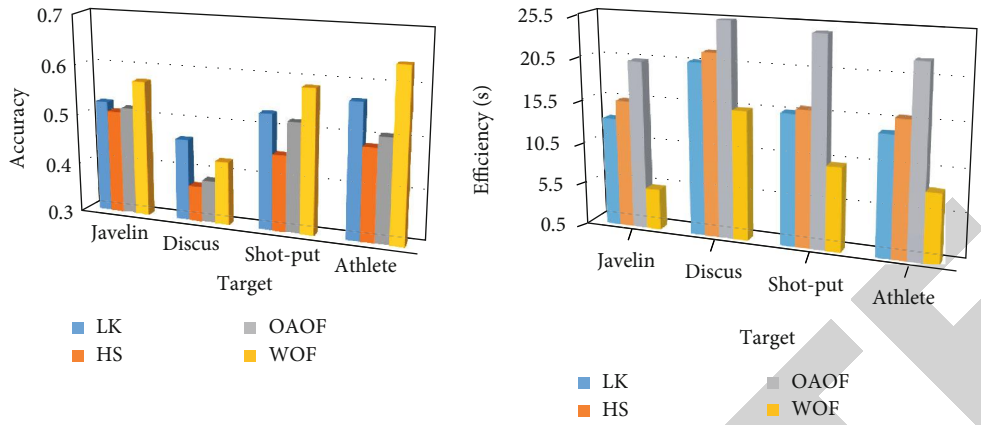

(a) Experimental results for the estimation accuracy

(b) Experimental results for algorithm efficiency

Figure 7: Accuracy of moving object estimation in moving image sequence.

continuous moving object detection between moving image interval frames. RWS algorithm through the whole scan determines the moving target detection results; in the process of scanning, RW of each translation n pixels in every direction, in order to detect moving targets of different size and overall scanning, will join a rectangular window scanning algorithm testing factor r; r can adaptively adjust according to the size of the moving target. The whole scanning process is repeated on the moving image until the size of RW is less than its corresponding r.

For the remaining overall scanning area of concern, the final detection area of the moving target is

$$\mathrm{RWS} = \sum\sum\left(H_{F(i,j-1)} - G_{F(i,j)} + L_{F(i,j)}\right). \tag{16}$$

4. Results and Discussion

The experiment in this paper is carried out on Windows platform, using Matlab2015B simulation platform. The computer has an Intel CPU, 16 GB memory, and 512 GB storage. The range of the experimental fuzzy scale L is set to [5, 60], and the range of the fuzzy angle θ is set to [0, 180].

The data sets used in this paper are all videos of open competitions, which are downloaded from the Internet using Python crawler technology.

4.1. Performance Analysis of Deblurring Algorithm. Firstly, the motion fuzzy of fuzzy scale ($5 \le L \le 60$) and fuzzy angle ($0^\circ \le \theta \le 180^\circ$) without noise were quantitatively analysed, and the absolute error results are shown in Figure 4. In Figure 4(a), fuzzy scale remains unchanged and absolute error of fuzzy angle. In Figure 4(b), fuzzy scale remains unchanged and fuzzy angle absolute error.

In order to further verify the reliability of DA algorithm, motion blur of different fuzzy scale ($5 \le L \le 30$) and different fuzzy angle ($0^\circ \le \theta \le 90^\circ$) was performed on three kinds of images. Gaussian noise with no noise and with noise (mean average = 0, mean variance = 0.001, Gaussian noise with mean variance = 0.00001) was quantitatively analysed, and fuzzy kernel and absolute error results were obtained, as shown in Tables 1–3.

Combined with the results of Figure 4 and Tables 1–3, the DA algorithm shows that without noise, the absolute error range of fuzzy angle is about 0-1.3, and the fuzzy scale is about 0-0.8. In the case of noise (Gaussian noise with mean value of 0 and mean square error of 0.001), the absolute error range of fuzzy angle is about 0-9.5, and the fuzzy scale is about 0-1.1. In the case of noise (Gaussian noise with mean value of 0 and mean square error of 0.00001), the absolute error range of fuzzy angle is about 0-1.3, and the fuzzy scale is about 0-0.8. It can be seen that the larger the fuzzy angle and fuzzy scale, the higher the accuracy of fuzzy kernel estimation. Therefore, the fuzzy kernel estimation algorithm based on spectrum characteristics has certain feasibility and relatively high accuracy.

4.2. Performance Analysis of Segmentation Algorithm. In order to measure the advantages and disadvantages of the video image character segmentation method, 100 video image character segmentation experiments were carried out, respectively, under the condition of no noise and added noise, and the obtained intraregion consistency measurement results are shown in Figure 5.

Figure 5 shows that the measure value deviating from the mean curve of consistency measure in the region is the abnormal measure value, which needs to be deleted in the calculation process. Through comparative study, it is found that the average value of intraregion consistency measure in the case of no noise is higher than that in the case of adding noise and generally higher than the standard value of 4.00, indicating the intraregion consistency measure result of this method. Therefore, it can be seen that the proposed algorithm has certain feasibility and good robustness.

This section compares the MEPSA algorithm with the classical segmentation algorithm. Among them, classical segmentation algorithms include pulse-coupled neural network (PCNN) [19], fuzzy neural network (FNN) [20], Gaussian SVM [21], and linear discriminant analysis (LDA) [22]. The specific comparison of segmentation results is shown in Figure 6.

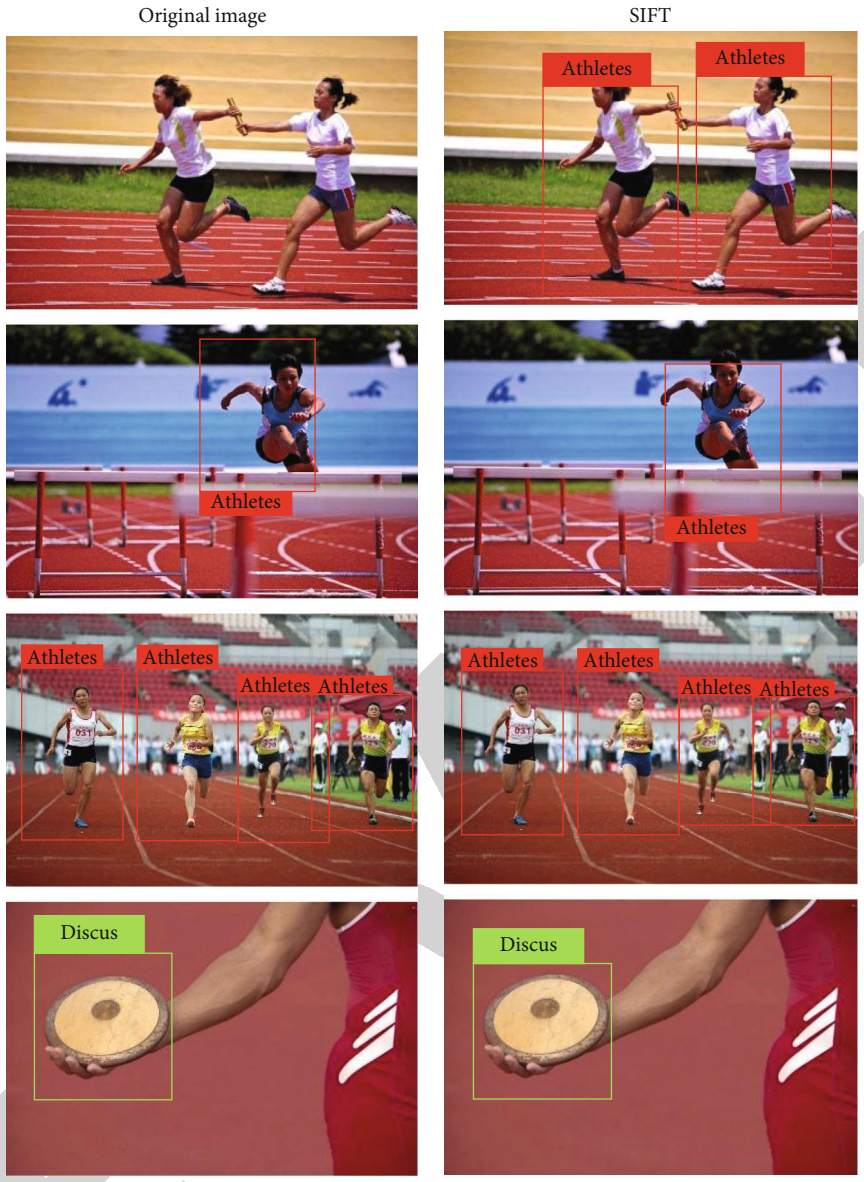

(a) Original image (b) SIFT

Figure 8: Continued.

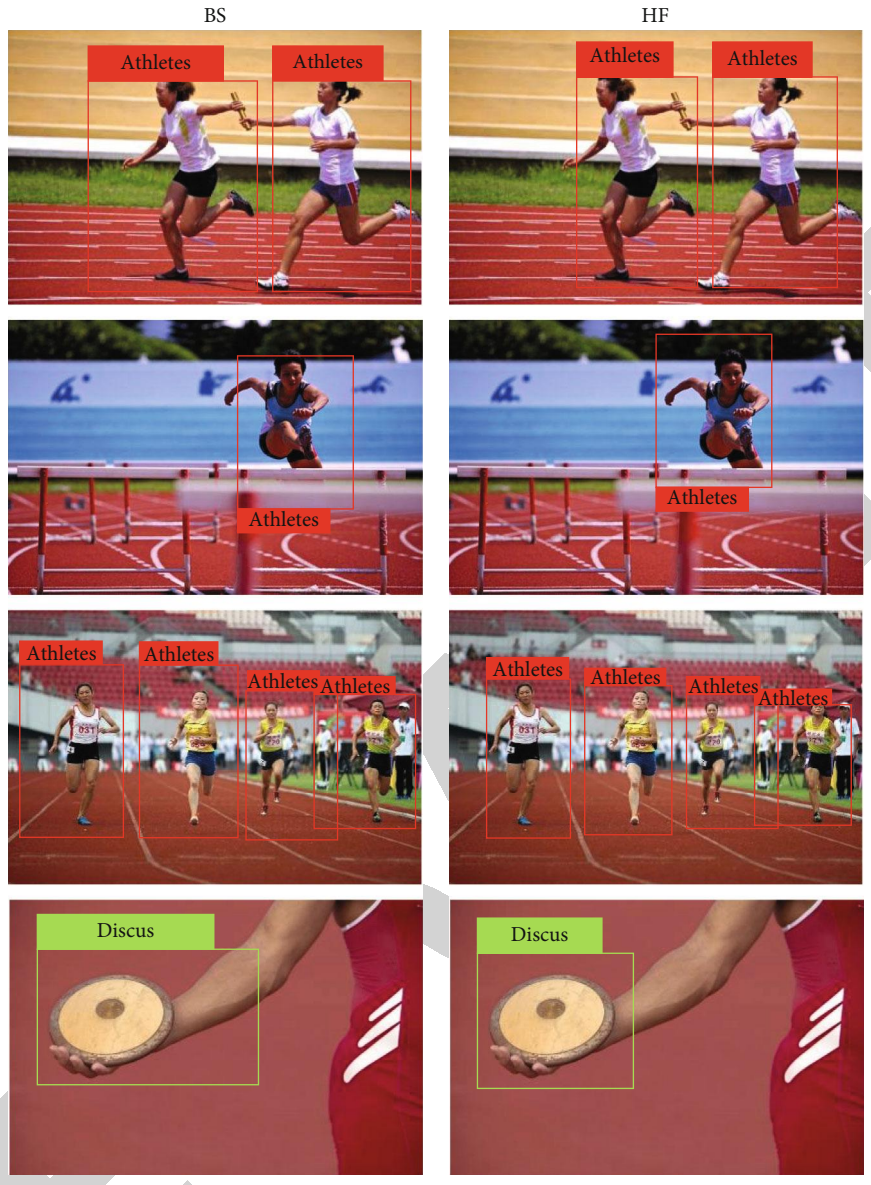

(c) BS (d) HF

Figure 8: Continued.

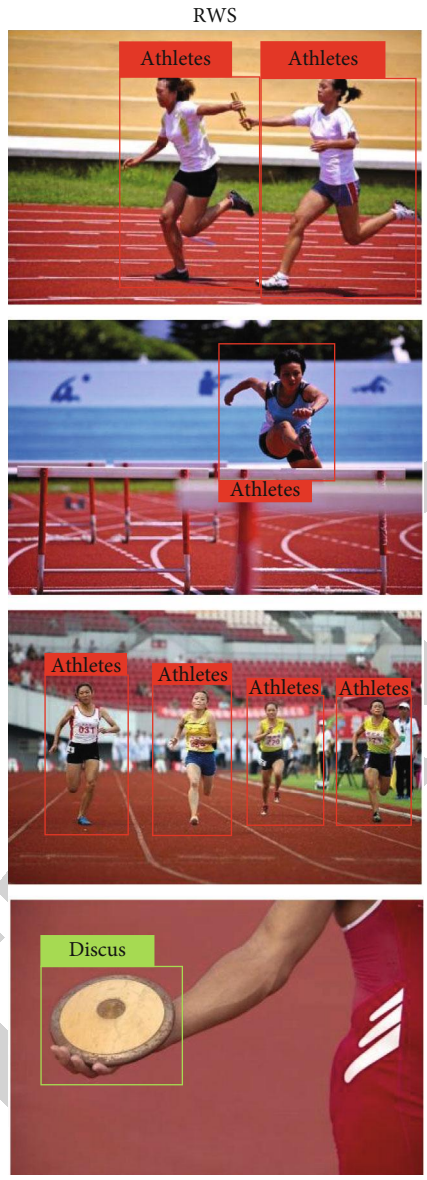

(e) RWS

Figure 8: Experimental results of moving images.

The experimental results show that the difference between different segmentation algorithms is obvious, and the neural network algorithm (PCNN and FNN) uses the grey entropy and threshold characteristics to calculate, which will cause diffusion at the edge of the moving target and result in large deviation. The GVSM algorithm does not use PCA to perform segmentation calculation directly, and the segmentation effect is better. The normalized value of MEPSA is obviously better than that of LDA. Compared with PCNN and FNN, MEPSA improved the segmentation accuracy by 20.6% and the normalized value by 15.1%. Compared with GVSM, MEPSA improves the normalization value by more than 5.19% and the segmentation accuracy by 4.91%. Compared with LDA, MEPSA improves the normalization value of more than 2.59% and the segmentation accuracy of 2.77%.

4.3. Performance Analysis of Detection Algorithm. In this section, the motion estimation performance of WOF was compared with the Lucas-Kanade (LK) [23], Horn-Schunck (HS) [24], and occlusion-aware optical flow (OAOF) [25].

The experimental results in Figure 7(a) show that compared with LK, WOF can improve the estimation accuracy by more than 10.4%. Compared with HS, the estimation accuracy can be improved by 13.6%. Compared with OAOF, it can improve the estimation accuracy by 12.7%. WOF makes use of the cross-scale property of wavelet transform to estimate the moving target continuously between different moving image sequences. WOF can adjust the moving target estimation adaptively according to the speed of the moving target, and the use of fuzzy features is helpful to improve the accuracy of the moving target estimation between different moving image sequences. Compared with LK, HS, and

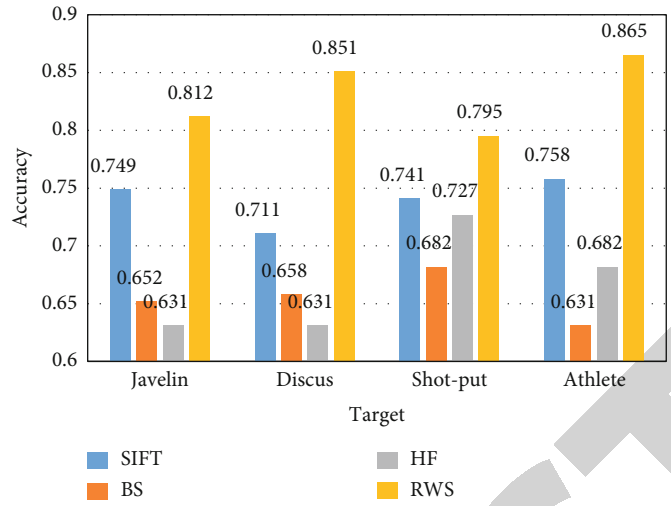

(a) Experimental results for the accuracy of motion target detection

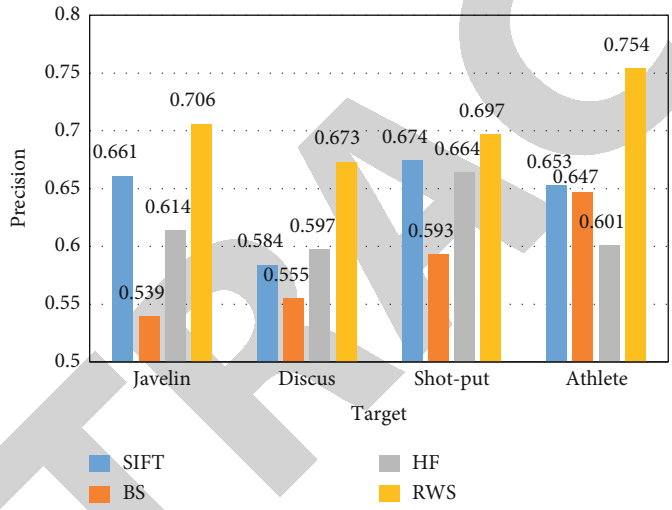

(b) Experimental results for the precision of motion target detection

Figure 9: Experimental results of moving target detection.

OAOF, the moving object estimation result obtained by WOF is closer to the real moving object trajectory.

Figure 7(b) compares the efficiency of the four algorithms. Due to the similar motion estimation process, the time difference between LK algorithm and HS algorithm is almost the same. OAOF will perform iterative optimization on the results of optical flow estimation in a specific interval, which takes longer time. WOF proposed in this paper can perform optical flow calculation at different frequencies in parallel. Compared with LK and HS, WOF can shorten the calculation time by 5-7 seconds, and compared with OAOF, WOF can shorten the calculation time by 10-14 seconds.

RWS proposed in this paper was also verified and compared on moving images. Figure 8 shows the experimental results of the rectangular window scanning algorithm. Among them, the comparison algorithm includes SIFT [26], background subtraction (BS) [27], and Hough forests (HF) [28].

It can be seen from the experimental results that the RWS proposed in this paper can detect the moving target with large volume in the close view and the moving target with small volume in the long view simultaneously, while SIFT, BS, and HF can only detect the moving target with large volume in the close view. This is mainly because after the iterative processing of the whole scanning of RWS, the basic loss of moving image has been made up, and the contrast of the detection result of moving target has been improved compared with the original moving image frame. SIFT detection results will deviate with the change of moving target speed. The experimental results of BS and HF also have some visual errors. RWS can automatically compensate the error generated in the recursive process.

In this section, three different objective indicators are used to evaluate the moving target detection performance of RWS, SIFT, BS, and HF. The experimental results are shown in Figure 9.

Compared with SIFT, RWS can improve the accuracy of target detection by 3.41%. Compared with BS, RWS can improve the target detection accuracy by 17.5%. Compared with HF, RWS can improve the target detection accuracy

by 4.97%. If the moving target detection results in different scenes are considered, RWS also has good universality. According to the experimental results of moving image sequence target detection, if the moving target activity region in the foreground is large, then the compensation region that can be improved in algorithm detection is also large. For moving objects in small areas, the detection results of moving objects after image compensation reconstruction will not be greatly affected. The objective evaluation experiment results of moving target detection can confirm that the RWS proposed in this paper has good moving target detection performance and can provide accurate moving target detection results.

5. Conclusion

To better serve track and field practice of the scientific and to utilize the motion video image processing technology to better guide and evaluate technique ability, a motion video image acquisition system is constructed. Secondly, a fuzzy kernel estimation method for uniform linear motion based on cepstrum property is proposed. The algorithm can detect the fuzzy region and clear region accurately from the local motion blurred image and mark the fuzzy region, so as to deblur the local motion blurred image. Then, the motion blur areas to be processed are selected, and only these areas are deblurred. Finally, the effective removal of local motion blur is realized, and a clear scene image is obtained. Then, a video image segmentation method based on maximum entropy threshold processing algorithm is proposed. The maximum value of the total entropy of the image is calculated by using the information entropy theory, and the particle swarm optimization algorithm is introduced to find the maximum threshold of image segmentation. Finally, a multiscale moving image target detection algorithm based on WOF and RWS is proposed, which solves the problem that the detection accuracy of fast moving targets is reduced by traditional optical flow estimation and improves the efficiency of optical flow calculation. Compared with other algorithms, the algorithm can improve the accuracy and precision of moving target detection.

In order to further improve the accuracy of target detection, timing information is considered in the next step of this paper. By adding timing information, the target is tracked, and the same target can be detected in multiple videos.

Data Availability

The data used to support the findings of this study are available from the corresponding author upon request.

Conflicts of Interest

The authors declare that they have no known competing financial interests or personal relationships that could have appeared to influence the work reported in this paper.

Acknowledgments

This work was supported by the College of Physical Education, Taiyuan University of Technology.

References

[1] Z. Yanpeng, "Hybrid kernel extreme learning machine for evaluation of athletes' competitive ability based on particle swarm optimization," *Computers and Electrical Engineering*, vol. 73, pp. 23–31, 2019.

[2] M. Kosaka, J. Nakase, H. Numata et al., "Psychological traits regarding competitiveness are related to the incidence of anterior cruciate ligament injury in high school female athletes," *The Knee*, vol. 23, no. 4, pp. 681–685, 2016.

[3] D. Calvo, P. González, L. Díaz et al., "A multi-processing systems-on-chip native simulation framework for power and thermal-aware design," *Journal of Low Power Electronics*, vol. 7, no. 1, pp. 2–16, 2011.

[4] P. Martinez and E. Villar, "Positioning system for recreated reality applications based on high-performance video-processing," in *Model-Implementation Fidelity in Cyber Physical System Design*, pp. 201–230, Springer, Cham, 2017.

[5] C. B. Moon, B. M. Kim, and D. S. Kim, "Real-time parallel image-processing scheme for a fire-control system," *IEIE Transactions on Smart Processing & Computing*, vol. 8, no. 1, pp. 27–35, 2019.

[6] S. Wang, S. Zhang, X. Huang, and L. Chang, "Single-chip multi-processing architecture for spaceborne SAR imaging and intelligent processing," *Xibei Gongye Daxue Xuebao/Journal of Northwestern Polytechnical University*, vol. 39, no. 3, pp. 510–520, 2021.

[7] T. Hussain, "ViPS: a novel visual processing system architecture for medical imaging," *Biomedical Signal Processing and Control*, vol. 38, pp. 293–301, 2017.

[8] A. Klilou and A. Arsalane, "Parallel implementation of pulse compression method on a multi-core digital signal processor," *International Journal of Electrical and Computer Engineering*, vol. 10, no. 6, pp. 6541–6548, 2020.

[9] X. Zhu, S. Cohen, S. Schiller, and P. Milanfar, "Estimating spatially varying defocus blur from a single image," *IEEE Transactions on Image Processing*, vol. 22, no. 12, pp. 4879–4891, 2013.

[10] W. Ren, X. Cao, J. Pan, X. Guo, W. Zuo, and M. H. Yang, "Image deblurring via enhanced low-rank prior," *IEEE Transactions on Image Processing*, vol. 25, no. 7, pp. 3426–3437, 2016.

[11] Q. Feng, L. Chen, C. L. P. Chen, and L. Guo, "Deep fuzzy clustering - a representation learning approach," *IEEE Transactions on Fuzzy Systems*, vol. 28, no. 7, pp. 1–1433, 2020.

[12] K. Gong, J. Cheng-Liao, G. Wang, K. T. Chen, C. Catana, and J. Qi, "Direct patlak reconstruction from dynamic PET data using the kernel method with MRI information based on structural similarity," *IEEE Transactions on Medical Imaging*, vol. 37, no. 4, pp. 955–965, 2018.

[13] A. Ibrahim and E. S. M. El-kenawy, "Image segmentation methods based on superpixel techniques: a survey," *Journal of Computer Science and Information Systems*, vol. 15, no. 3, pp. 1–11, 2020.

[14] H. Yu, F. He, and Y. Pan, "A scalable region-based level set method using adaptive bilateral filter for noisy image segmentation," *Multimedia Tools and Applications*, vol. 79, no. 9-10, pp. 5743–5765, 2020.

[15] X. Cao, S. Gao, L. Chen, and Y. Wang, "Ship recognition method combined with image segmentation and deep learning feature extraction in video surveillance," *Multimedia Tools and Applications*, vol. 79, no. 13-14, pp. 9177–9192, 2020.

[16] Z. Tu, W. Xie, D. Zhang et al., "A survey of variational and CNN-based optical flow techniques," *Signal Processing: Image Communication*, vol. 72, pp. 9–24, 2019.

[17] T. W. Hui, X. Tang, and C. C. Loy, "A lightweight optical flow CNN—revisiting data fidelity and regularization," *IEEE Transactions on Pattern Analysis and Machine Intelligence*, vol. 43, no. 8, pp. 2555–2569, 2021.

[18] M. Zhai, X. Xiang, R. Zhang, N. Lv, and A. el Saddik, "Optical flow estimation using dual self-attention pyramid networks," *IEEE Transactions on Circuits and Systems for Video Technology*, vol. 30, no. 10, pp. 3663–3674, 2020.

[19] J. Lian, Z. Yang, J. Liu et al., "An overview of image segmentation based on pulse-coupled neural network," *Archives of Computational Methods in Engineering*, vol. 28, no. 2, pp. 387–403, 2021.

[20] K. Zheng, Q. Zhang, Y. Hu, and B. Wu, "Design of fuzzy system-fuzzy neural network-backstepping control for complex robot system," *Information Sciences*, vol. 546, pp. 1230–1255, 2021.

[21] T. M. Ghazal, "Hep-pred: hepatitis c staging prediction using fine Gaussian SVM," *Computers, Materials & Continua*, vol. 69, no. 1, pp. 191–203, 2021.

[22] M. Esteki, Z. Shahsavari, and J. Simal-Gandara, "Use of spectroscopic methods in combination with linear discriminant analysis for authentication of food products," *Food Control*, vol. 91, pp. 100–112, 2018.

[23] S. Yao, X. Han, H. Zhang, X. Wang, and X. Cao, "Learning deep Lucas-Kanade Siamese network for visual tracking," *IEEE Transactions on Image Processing*, vol. 30, pp. 4814–4827, 2021.

[24] M. Nadour, M. Boumehraz, L. Cherroun, and V. Puig Cayuela, "Hybrid type-2 fuzzy logic obstacle avoidance system based on horn-schunck method," *Electrotehnica, Electronica, Automatica*, vol. 67, no. 3, pp. 45–51, 2019.

[25] A. Holynski and J. Kopf, "Fast depth densification for occlusion-aware augmented reality," *ACM Transactions on Graphics (ToG)*, vol. 37, no. 6, pp. 1–11, 2018.

[26] K. Xia, H. Yin, and Y. Zhang, "Deep semantic segmentation of kidney and space-occupying lesion area based on SCNN and ResNet models combined with SIFT-flow algorithm," *Journal of Medical Systems*, vol. 43, no. 1, pp. 1–12, 2018.

[27] T. Bouwmans, S. Javed, M. Sultana, and S. K. Jung, "Deep neural network concepts for background subtraction:a systematic review and comparative evaluation," *Neural Networks*, vol. 117, pp. 8–66, 2019.

[28] I. Serrano, O. Deniz, J. L. Espinosa-Aranda, and G. Bueno, "Fight recognition in video using hough forests and 2D convolutional neural network," *IEEE Transactions on Image Processing*, vol. 27, no. 10, pp. 4787–4797, 2018.